Intramyocardial injection of hypoxia-conditioned extracellular vesicles modulates apoptotic signaling in chronically ischemic myocardium

Check for updates

Dwight D. Harris, MD, Sharif A. Sabe, MD, Mohamed Sabra, MD, Cynthia M. Xu, MD, Akshay Malhotra, Mark Broadwin, MD, Debolina Banerjee, MD, M. Ruhul Abid, MD, PhD, and Frank W. Sellke, MD

ABSTRACT

Objective: Limited treatments exist for nonoperative chronic coronary artery disease. Previously, our laboratory has investigated extracellular vesicle (EV) therapy as a potential treatment for chronic coronary artery disease using a swine model and demonstrated improved cardiac function in swine treated with intramyocardial EV injection. Here, we seek to investigate the potential cardiac benefits of EVs by using hypoxia-conditioned EVs (HEV). Specifically, this study aims to investigate the effect of HEV on apoptosis in chronically ischemic myocardium in swine.

Methods: Fourteen Yorkshire swine underwent placement of an ameroid constrictor on the left circumflex artery. Two weeks later, swine underwent redo left thoracotomy with injection of either saline (control, n = 7) or HEVs (n = 7). After 5 weeks, swine were euthanized for tissue collection. Terminal deoxynucleotidyl transferase dUTP nick end labeling was used to quantify apoptosis. Immunoblotting was used for protein quantification.

Results: Terminal deoxynucleotidyl transferase dUTP nick end labeling staining showed a decrease in apoptosis in the HEV group compared with the control ($P = .049$). The HEV group exhibited a significant increase in the anti-apoptotic signaling molecule phospho-BAD ($P = .005$), a significant decrease in B-cell lymphoma 2 ($P = .006$) and an increase in the phospho-B-cell lymphoma to B-cell lymphoma 2 ratio ($P < .001$). Furthermore, the HEV group exhibited increased levels of prosurvival signaling markers including phosphoinositide 3-kinase, phosphor-extracellular signal-regulated kinase 1/2, phospho-forkhead box protein O1, and phospho-protein kinase B to protein kinase B ratio (all $P < .05$).

Conclusions: In chronic myocardial ischemia, treatment with HEV results in a decrease in overall apoptosis, possibly through the activation of both pro-survival and anti-apoptotic signaling pathways. (JTCVS Open 2023;15:220-8)

Hypoxia-condition EV

100 μm
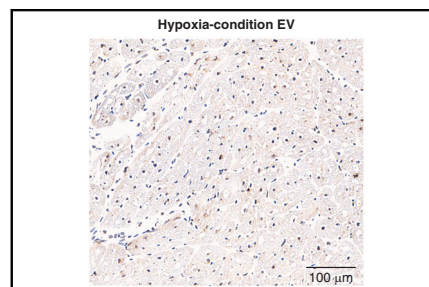
TUNEL stain shows a decrease in total apoptosis in the hypoxia EV group.

CENTRAL MESSAGE

Intramyocardial injection of hypoxia-conditioned extracellular vesicles results in decreased overall apoptosis, which is associated with an increase in key antiapoptotic and cell survival markers.

PERSPECTIVE

Limited treatments exist for nonoperative chronic coronary artery disease. Intramyocardial injection of hypoxia-conditioned extracellular vesicles (HEVs) has been shown to increase cardiac function, and our study suggests decreasing apoptosis could play a role in the cardiac benefits seen with HEV injection. HEVs could represent a novel therapy for the management of advanced coronary artery disease.

AKT	=	protein kinase B
Bcl-2	=	B-cell lymphoma 2
CAD	=	coronary artery disease
CON	=	control saline injection
ERK	=	extracellular signal-regulated kinase 1/2
EV	=	extracellular vesicle
FAK	=	focal adhesion kinase
FOXO1	=	forkhead box protein O1
HBMSC	=	human bone marrow–derived stem cell
HEV	=	hypoxia-conditioned extracellular vesicle
LCx	=	left circumflex artery
P90RSK	=	90-kDa ribosomal s6 kinases
pAKT	=	phospho-protein kinase B
pBAD	=	phospo-Bcl-2–associated death promoter-serine 112
pBcl-2	=	phospho-B-cell lymphoma 2
pERK	=	phospho-extracellular signal-regulated kinase 1/2
pFOXO1	=	phospho-forkhead box protein O1
PI3K	=	phosphoinositide 3-kinase
pP90RSK	=	phospho-90-kDa ribosomal s6 kinases
TBST	=	tris-buffered saline
TUNEL	=	terminal deoxynucleotidyl transferase dUTP nick end labeling

▶ Video clip is available online.

To view the AATS Annual Meeting Webcast, see the URL next to the webcast thumbnail.

Despite being a major contributor to global mortality, there are few effective medical treatments available for end-stage coronary artery disease (CAD) that cannot be managed with surgical or endovascular intervention.[1] Without proper treatment, atherosclerotic CAD continues to progress and may result in congestive heart failure or acute infarction.[2,3]

Extracellular vesicles (EVs) are membrane-bound structures that are released by cells into the extracellular environment.[4] EVs contain a variety of biological molecules, including proteins, cytokines, lipids, and nucleic acids.[4] Numerous studies have shown that EVs play a crucial role in intercellular communication and regulation of molecular pathways.[4-7] In light of recent studies, EVs have emerged as promising candidates for novel therapeutic targets in cardiovascular diseases.[6] Small-animal rodent models have shown increased cardiac function and modulation of cardiac inflammation with EV injection.[8] Furthermore, our group has previously demonstrated increased cardiac function and decreased inflammation using a large-animal swine model of chronic myocardial ischemia without significant changes in apoptotic signaling.[9-11] Other animal studies have shown that EVs play a crucial role in cardiac function, angiogenesis, cardiac regeneration, inflammation, and myocardial remodeling.[12]

Traditional EVs are collected from human bone marrow–derived stem cells (HBMSCs) that are grown under normoxia. However, progenitor cells, such as HBMSC, that produce EVs can be preconditioned to alter the properties and components of EVs.[13] For instance, hypoxia can alter the composition and function of EVs released by cells. Hypoxia-conditioned extracellular vesicles (HEVs) are enriched in various bioactive molecules that promote cell survival and adaptation to low-oxygen environments.[14,15] This is of particular interest in chronic myocardial ischemia, as chronic ischemia results in a low oxygen environment in the affected tissues. HEVs have been shown to decrease infarct size and overall apoptosis in a mouse model of acute myocardial ischemia/reperfusion.[15] However, studies involving large animals to evaluate the use of HEVs in myocardial ischemia are limited. To fill this research gap, our group elected to study HEVs using our large animal model for chronic myocardial ischemia. The use of HEVs by our group has been extensively studied with electron microscopy, immunoblotting, and total proteomic analysis.[16] Total proteomic analysis has demonstrated proteins important for transport, calcium handling, redox, and metabolism pathways.[16] Our group has previously demonstrated enhanced contractility, capillary density, and angiogenic signaling pathways in HEVs compared to traditional normoxia serum-starved EVs using HEVs in a swine model for chronic myocardial ischemia.[10] It appears that HEVs offer significant improvement in cardiac function, but the mechanism remains unclear. Therefore, we seek to further understand the cardiac benefits of HEVs by studying the effect for HEVs on apoptosis in a swine model of chronic myocardial ischemia.

METHODS
Model
Fourteen eleven-week-old Yorkshire swine (Cummings School of Veterinary Medicine of Tufts University Farm) underwent left thoracotomy and placement of an ameroid constrictor (Research Instruments SW) on the left circumflex artery (LCx) to model chronic CAD. Two weeks later, swine underwent redo left thoracotomy with injection of either normal saline (CON, n = 7) or HEVs (n = 7). Five weeks after injection, swine were euthanized for tissue collection (Video 1 and Figure 1).
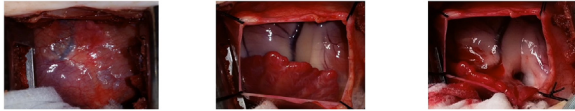
VIDEO 1. Methods. Fourteen 11-week-old Yorkshire swine underwent left thoracotomy and placement of an ameroid constrictor on the left circumflex artery (LCx). Extracellular vesicles where cultured, hypoxia conditioned, and collected. Two weeks later, swine underwent redo left thoracotomy with injection of either normal saline (CON, n = 7) or hypoxia-conditioned extracellular vesicles HEVs (n = 7). Five weeks after injection, swine were euthanized for tissue collection. Video available at: https://www.jtcvs.org/article/S2666-2736(23)00163-8/fulltext.

Humane Animal Care

All animals received humane care in compliance with the Guide for the Care and Use of Laboratory Animals. All experiments were approved by the local Institutional Animal Care and Use Committee.

Ameroid

Anesthesia and preoperative care were performed as previously reported.[17] A left thoracotomy was performed in the second intercostal space as previously described.[17] The pericardium was opened, then blunt and sharp dissection were used to expose the LCx and left anterior descending artery. The LCx was traced back to its origin from the left main coronary artery. After adequate exposure was obtained, the swine was given intravenous heparin (80 IU/kg), and a vessel loop was placed around the LCx. The LCx was occluded for 2 minutes by lifting the vessel loop. Five milliliters of gold microspheres (BioPal) were injected into the left atrium during LCx occlusion to map the area of ischemia.[17] The ameroid was then placed on the LCx as close as possible to the bifurcation of the LCx from the left main coronary artery to create a consistent ischemic area. The pericardium was filled with 5 mL of normal saline and closed with absorbable suture. The chest was closed in layers as previously described. The skin was closed with MONOCRYL suture and dressed with betadine-soaked gauze and Tegaderm (3M).

EV Collection

HBMSCs (Lonza) were cultured according to Lonza recommendations in growth media (MSCGM Bulletkit PT-3001; Lonza) as previously described.[10] HBMSCs were grown to 80% confluence and passaged to passage 7. At this point, the media was replaced with MSCGM media, and cells were placed in a humidified hypoxia chamber (Billups-Rothenberg, MIC-101) containing 5% carbon dioxide and 95% nitrogen.[10] The cells were incubated for 24 hours at 37 °C. After 24 hours, the hypoxia chambers
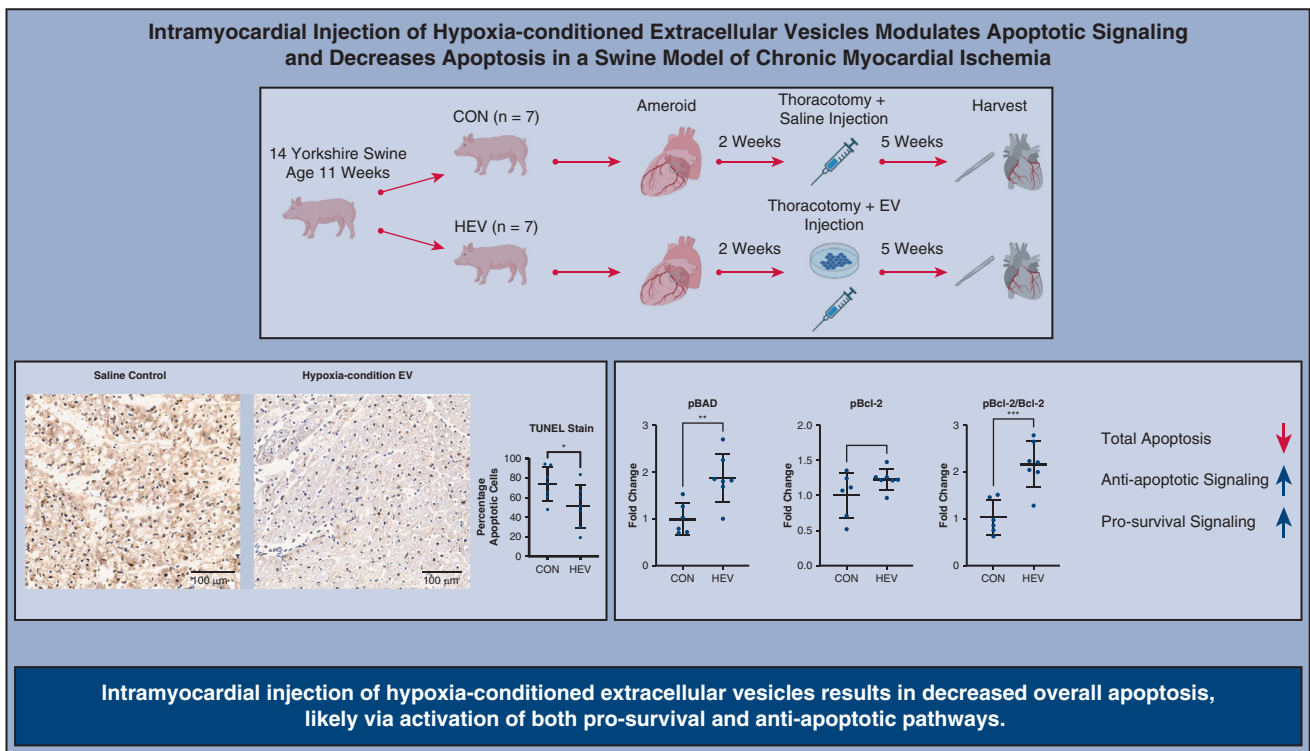
FIGURE 1. Fourteen swine were assigned to 2 groups: saline control injection (*CON*) or hypoxia-conditioned extracellular vesicles (*HEV*). Swine underwent placement of an ameroid constrictor on the left coronary circumflex artery at age 11 weeks. Two weeks later, all swine underwent redo-left thoracotomy with injection of CON or HEV. Terminal deoxynucleotidyl transferase dUTP nick end labeling (*TUNEL*) stain showed a decrease in total apoptosis in the HEV group compared with control. Immunoblotting showed increased concentration of prosurvival and antiapoptotic proteins. Intramyocardial injection of hypoxia-conditioned extracellular vesicle results in decreased overall apoptosis, likely via activation of both prosurvival and antiapoptotic pathways. *EV*, Extracellular vesicles; *pBAD*, phospo-Bcl-2–associated death promoter-serine 112; *pBcl-2*, phospho-B-cell lymphoma 2; *Bcl-2*, B-cell lymphoma 2. *$P < .05$, **$P < .01$, ***$P < .001$.

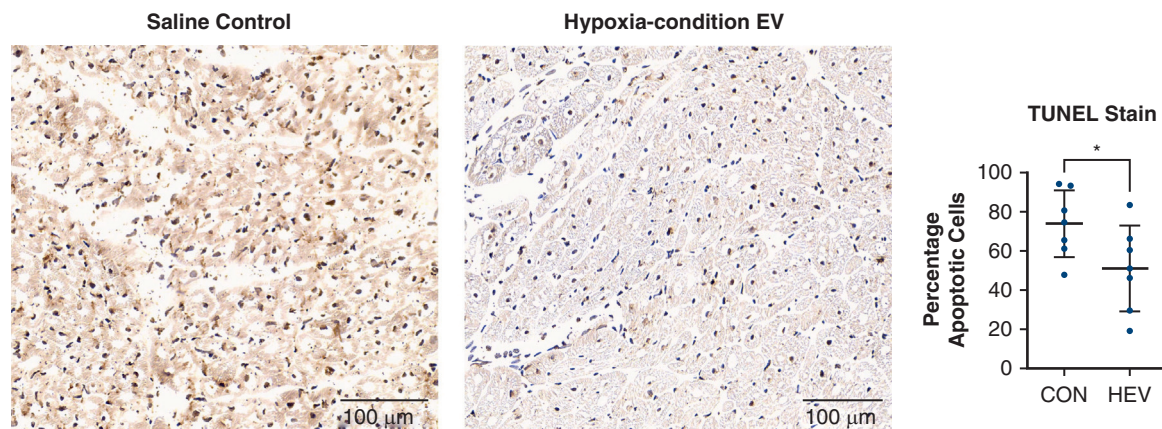**FIGURE 2.** TUNEL staining. Terminal deoxynucleotidyl transferase dUTP nick end labeling (*TUNEL*) stain shows a decrease in total apoptosis in the hypoxia-conditioned extracellular vesicles (*HEV*, n = 7) compared with saline control (*CON*, n = 7). *Graphs* represent data points mean with standard deviation. *EV*, Extracellular vesicles. *P < .05.

were opened. The media was collected and the EVs were isolated from the media as previously described.[10] The EVs were characterized with electron microscopy, nanoparticle tracking analysis and immunoblotting, as previously described and published.[10,16] Protein quantification was performed using a radioimmunoprecipitation assay (Kit 23225; Thermo Fisher Scientific) in order to verify a standard dose for intramyocardial injection.[10]

EV Injection

EVs (50 µg) were thawed and mixed in 2 mL of 0.9% sterile saline on the day of injection. Anesthesia and preoperative care were performed as previously reported.[17] A left thoracotomy was performed one rib space below the prior surgical site. Sharp and blunt dissection were used to enter the thoracic cavity and take down pulmonary adhesions. The pericardium was opened and secured with silk suture. The myocardium was injected in ten locations adjacent to the LCx territory.[10] The pericardium was closed with absorbable suture, and the chest was closed as described above.

Tissue Harvest

Anesthesia and preoperative care were performed as previously reported.[17] The swine was placed supine and prepped with betadine. A median sternotomy was performed, followed by adhesiolysis. The pericardium was opened and the heart was dissected free from tethering scar tissue. Physiologic measurements were conducted as previously reported.[17] Anesthesia was deepened, and the heart was removed. The heart was sectioned into 16 segments and snap frozen in liquid nitrogen.

Terminal Deoxynucleotidyl Transferase dUTP Nick End Labeling (TUNEL) Staining

TUNEL staining was performed on frozen samples from the most ischemic area, defined using gold mapping at the time of ameroid placement, from seven control and seven experimental swine. The samples were stained and imaged by iHisto. Analysis for TUNEL staining was analyzed using QuPath software.[17] Three 10-mm² sections were selected per slide and analyzed using the QuPath automated detection program as previously described.[17] The TUNEL positive to negative nuclei ratio was calculated and averaged across the three 10-mm² sections.

Immunoblotting

Ischemic myocardial tissue from the same area used for TUNEL staining was lysed from 6 control animals and 7 experimental animals using RIPA Lysis and Extraction Buffer, Halt Protease Inhibitor Cocktail (Thermo Fisher Scientific), and an ultrasonic homogenizer.[17] Protein

TABLE 1. Apoptotic markers

Marker	HEV (mean ± standard deviation)	P
Proapoptotic		
AIF	1.03 ± 0.07	.69
BAX	0.93 ± 0.36	.76
Caspase-3	0.82 ± 0.18	.26
Caspase-9	0.82 ± 0.12	.44
FAK	0.98 ± 0.13	.83
FAS	1.01 ± 0.28	.94
FOXO1	0.97 ± 0.31	.87
Antiapoptotic		
pAKT	1.42 ± 0.55	.10
AKT	1.08 ± 0.31	.84
pAKT/AKT ratio	1.29 ± 0.23	**.04**
pBAD	1.87 ± 0.48	**.005**
Bcl-2	0.60 ± 0.17	**.006**
pBcl-2	1.23 ± 0.14	.12
pBcl-2/Bcl-2 ratio	2.64 ± 0.49	**<.001**
pERK	2.05 ± 1.19	.05
ERK	1.38 ± 0.37	**.008**
pERK/ERK ratio	1.47 ± 0.52	.18
pFOXO1	1.37 ± 0.15	**.04**
pFOXO1/FOXO1 ratio	1.53 ± 0.45	**.02**
IL-3	1.07 ± 0.06	.31
PI3K	1.53 ± 0.23	**.008**
pP90RSK	1.40 ± 0.25	.37
P90RSK	1.04 ± 0.28	.18
pP90RSK/P90RSK ratio	1.42 ± 0.39	.92

Shown are immunoblotting results for all markers tested in the study. Immunoblotting data are represented as mean fold change in hypoxia-conditioned extracellular vesicle group (HEV, n = 7) with standard deviation (SD) normalized to average control (n = 6). Data points greater than 2 standard deviations from the mean are excluded from analysis. P values less than .05 are shown in bold. *HEV*, Hypoxia-conditioned extracellular vesicle group; *AIF*, apoptosis-inducing factor; *BAX*, bcl-2-like protein 4; *FAK*, focal adhesion kinase; *FAS*, Fas cell surface Death receptor; *FOXO1*, forkhead box O1; *pAKT*, phospho-protein kinase B; *AKT*, protein kinase B; *pBAD*, phospho-Bcl-2-associated death promoter; *Bcl-2*, B-cell lymphoma 2; *pBcl-2*, phospho-B-cell lymphoma 2; *pERK*, phospho-extracellular signal-regulated kinase; *ERK*, extracellular signal-regulated kinase; *pFOXO1*, phospho-forkhead box O; *IL-3*, interleukin 3; *PI3K*, phosphoinositide 3-kinase; *pP90RSK*, phospho-p90 ribosomal S6 kinase; *P90RSK*, p90 ribosomal S6 kinase.
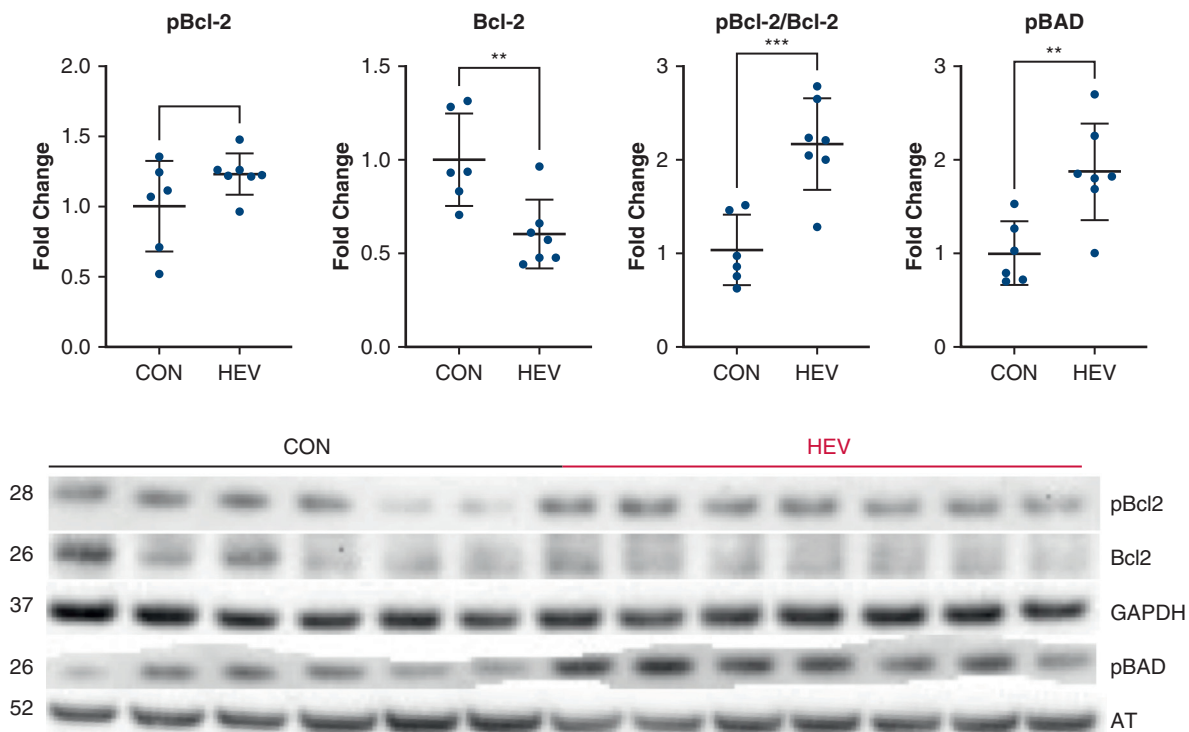
FIGURE 3. Antiapoptotic signaling. Immunoblotting showed a significant increase in concentration of anti-apoptotic Bcl-2-associated death promoter (*pBAD*) in the hypoxia-conditioned extracellular vesicle group (*HEV*, n = 7) compared with saline control (*CON*, n = 6). Phospho-B-cell lymphoma 2 (*pBcl-2*) showed a trend towards an increase in HEV treatment, and B-cell lymphoma 2 (*Bcl-2*) was significantly decreased with HEV treatment compared to CON. This resulted in a significant increase in the pBcl-2 to BCL-2 ratio in the HEV group. *Graphs* represent data points with mean with standard deviation. Immunoblotting data are -fold change normalized to average control. Data points greater than 2 standard deviations from the mean are excluded from analysis. *GAPDH*, Glyceraldehyde 3-phosphate dehydrogenase; *AT*, alpha-tubulin. **$P < .01$, ***$P < .001$.

concentration was calculated using a BCA Protein Assay Kit (Thermo Fisher Scientific). The lysate (40 μg) ran on a 4% to 12% Bis-Tris gel (Thermo Fisher Scientific) and was transferred to nitrocellulose (Thermo Fisher Scientific). Then, 5% non-fat dry milk in tris-buffered saline (TBST; Boston BioProducts) was used to block the membranes for 1 hour. The membranes were incubated for 24 hours with 1:1000 dilutions of primary antibodies in 3% bovine serum albumin in TBST based on the manufacture's recommendation. Horseradish peroxidase linked secondary antibodies to mouse or rabbit (Cell Signaling) were mixed as a 2.5:10,000 dilutions in 3% bovine serum albumin in TBST and the membranes were incubated for 1 hour at room temperature.[17] The membranes were imaged on a ChemiDoc Imaging System (Bio-Rad) using ECL Western Blotting Substrate (Thermo Fisher Scientific) developing agent. Membranes were stripped with Restore PLUS Western Blot Stripping Buffer (Thermo Fisher Scientific) to allow for repeat probing. Immunoblot data were analyzed using Image J software (National Institutes of Health).

Antibodies

Antibodies were selected base on literature review of key apoptotic pathways and availability of primary antibodies that react consistently with swine myocardium. Primary antibodies to apoptosis-inducing factor, phospho-protein kinase B–serine 473 (pAKT), protein kinase B (AKT), phospo-Bcl-2–associated death promoter-serine 112 (pBAD), bcl-2-like protein 4, B-cell lymphoma 2 (Bcl-2), phospho-B-cell lymphoma 2 (pBcl-2)–serine 70, caspase-3, caspase-9, phospho-extracellular signal-regulated kinase 1/2-threonine 202/204 (pERK), extracellular signal-

regulated kinase 1/2 (ERK 1/2), focal adhesion kinase, Fas (CD95 receptor), phospho-forkhead box protein O1-threonine 32 (pFOXO1), forkhead box protein O1-threonine 32 (FOXO1), phosphoinositide 3-kinases (PI3K), and 90-kDa ribosomal s6 kinases (P90RSK) were obtained from Cell Signaling. Primary antibodies to interleukin-3 and phospho-90 kDa ribosomal s6 kinases-threonine359/serine 363 (pP90RSK) were obtained from Proteintech.

Perfusion Analysis

Myocardial perfusion was determined by injection of isotope-labeled microspheres (Biophysics Assay Laboratory) at the time of the harvest procedure, as previously reported.[17] During the harvest procedure, 5 mL of lutetium and samarium microspheres were injected into the left atrium at rest and during pacing to 150 beats per minute, respectively, while simultaneously withdrawing 10 mL of blood from the femoral artery at reference rate of 6.67 mL/min using a withdrawal pump (Harvard Apparatus). Following euthanasia and tissue harvest, blood samples and left ventricular myocardial samples the ischemic myocardial territory was weighed, dried, and sent to Biophysics Assay laboratory for microsphere density measurements. Blood flow was calculated using the following equation: tissue blood flow = (reference blood flow [mL/min]/tissue weight [g]) $\times$ (tissue microsphere count/reference blood microsphere count).[17]

Statistical Analysis

All data was analyzed using Prism 9 (GraphPad Software). Shapiro–Wilk test was used to test for normality. Nonparametric data were analyzed with Wilcoxon rank-sum, and Student *t*-test was used to analyze normal
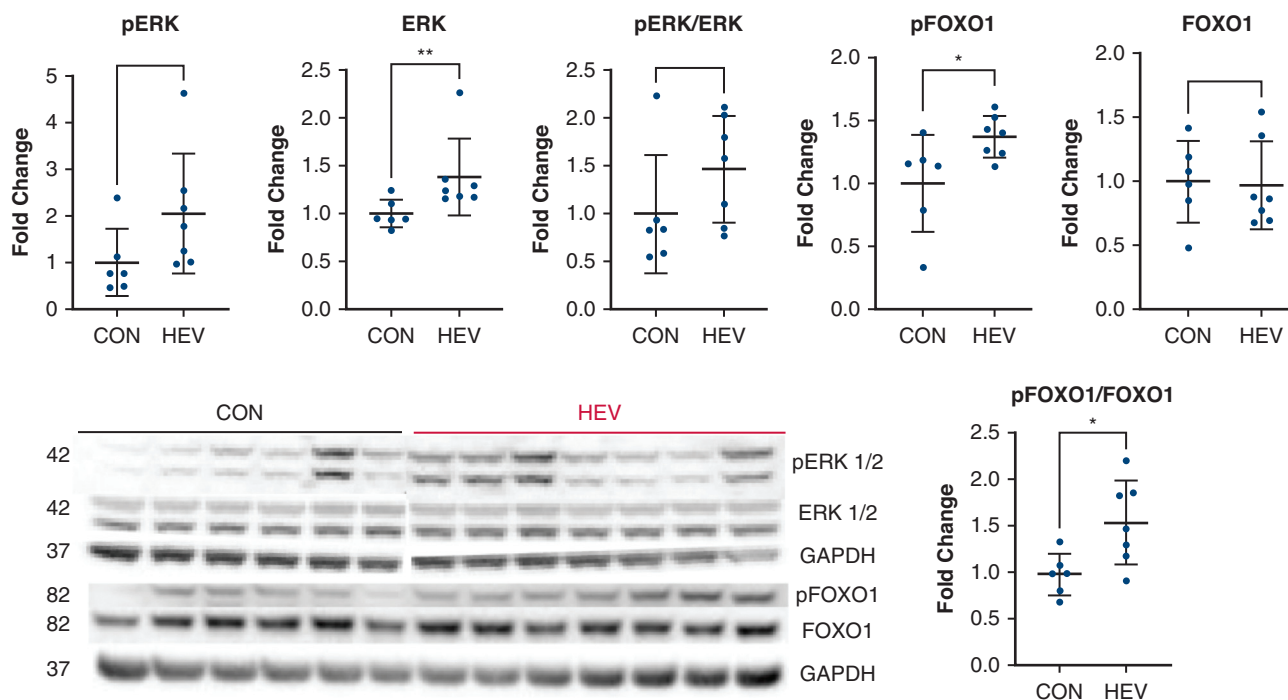
FIGURE 4. ERK and FOXO1 signaling. Immunoblotting showed a trend towards increased phospho-extracellular signal-regulated kinases (pERK) and a significant increase in extracellular signal-regulated kinases (ERK) in the hypoxia-conditioned extracellular vesicle group (*HEV*, n = 7) compared with the control group (*CON*, n = 6). There was a significant increase in the expression of phospho-forkhead box O1 (pFOXO1) and an increase in the pFOXO1 to forkhead box O1 (FOXO1) ratio. *Graphs* represent data points mean with standard deviation. Immunoblotting data are fold change normalized to average control. Data points greater than 2 standard deviations from the mean are excluded from analysis. *EV*, Extracellular vesicles; *TUNEL*, terminal deoxynucleotidyl transferase dUTP nick end labeling; *pBAD*, phospo-Bcl-2–associated death promoter-serine 112; *pBcl-2*, phospho-B-cell lymphoma 2; *Bcl-2*, B-cell lymphoma 2. *$P < .05$.

data. Data are represented as mean and standard deviation. Immunoblot data are represented as mean fold change normalized to the average control. Protein expression was plotted against our previously reported myocardial blood flow at rest and during pacing at 150 beats per minute, and analyzed using Spearman rank correlation coefficient.[10] Data points greater than 2 standard deviations from the mean were excluded from analysis.

RESULTS

TUNEL staining showed a significant decrease in total apoptosis in the HEV-treated ischemic myocardium compared with CON ischemic myocardium ($P = .049$) (Figure 2). There was a significant increase in pBAD ($P = .005$) in the HEV group compared with CON. There was a significant decrease is Bcl-2 ($P = .006$) and a trend towards increased pBcl-2 ($P = .12$) in the HEV group. This resulted in a significant increase in the ratio of pBcl-2 to Bcl-2 ($P < .001$) in the HEV group (Table 1 and Figure 3).

There was a significant increase in intermediate signaling molecule pERK ($P = .008$), and a strong trend towards increased ERK ($P = .05$) in the HEV group compared to CON. The HEV group had a significant increase in

pFOXO1 ($P = .04$), and a significant increase the pFOXO1 to FOXO1 ratio compared to the CON group ($P = .02$) (Figure 4). The HEV group had a significant increase in PI3K ($P = .008$) compared with the CON group. There was a trend towards an increase in pAKT ($P = .10$) and a significant increase in the pAKT to AKT ratio ($P = .04$) in the HEV group compared to CON (Figure 5).

There was a trend toward increased total P90RSK ($P = .33$) in the HEV group compared with CON. There were no significant changes in bcl-2-like protein 4, caspase-9, focal adhesion kinase, apoptosis-inducing factor, Fas, or interleukin-3 (all $P > .05$).

There was a positive correlation between ischemic myocardial flow at rest and the ratio of pAKT to AKT in the HEV group (r = 0.86, $P = .02$). In addition, there was a negative correlation between ischemic myocardial flow at rest and the expression of pBAD (r = 0.86, $P = .02$) in the HEV group. However, there was no significant correlation found with pBcl-2, Bcl-2, ERK, pFOXO1, FOXO1, or PI3K. There was no significant correlation between myocardial flow while pacing and the expression of any of the significant markers (Table 2)
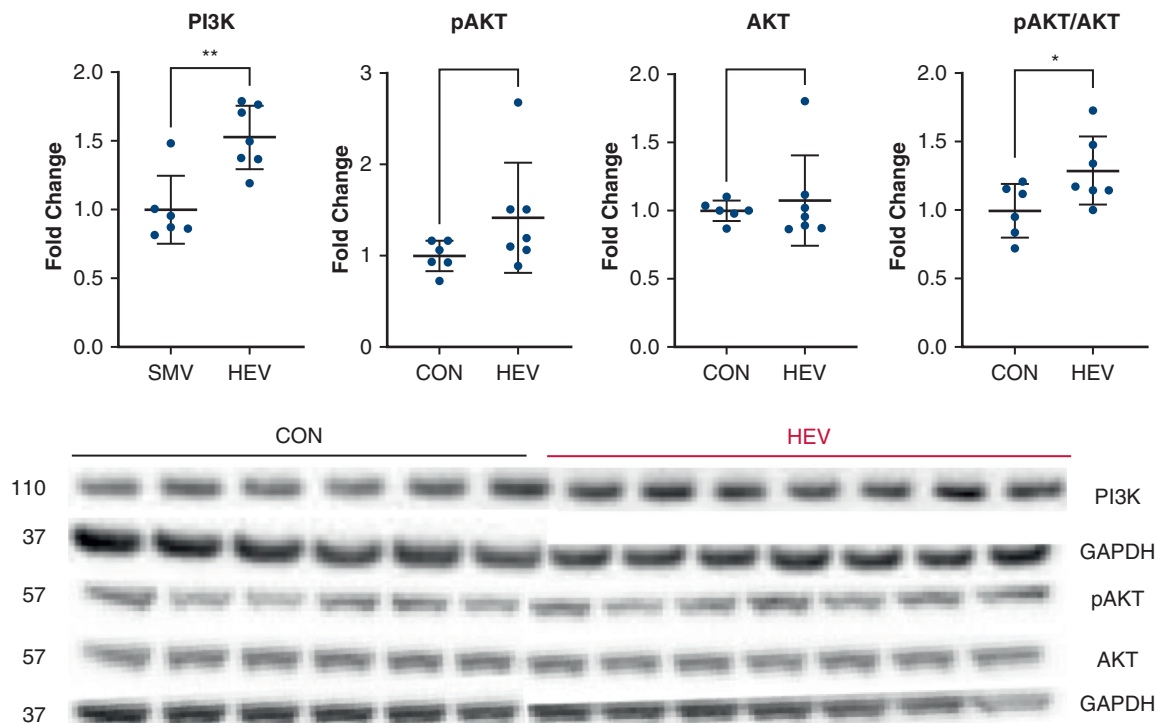
FIGURE 5. Phosphoinositide 3-kinase (*PI3K*) and protein kinase B (*AKT*) signaling. Immunoblotting showed a significant increase in PI3K expression in the hypoxia-conditioned extracellular vesicle group (*HEV*, n = 7) compared with saline control (*CON*, n = 6). There was a trend towards increased phospho-protein kinase B (*pAKT*) and a significant increase in the pAKT to AKT ratio in the HEV group compared with CON. *Graphs* represent data points mean with standard deviation. Immunoblotting data are fold change normalized to average control. Data points greater than 2 standard deviations from the mean are excluded from analysis. *GAPDH*, Glyceraldehyde 3-phosphate dehydrogenase. *$P < .05$, **$P < .01$.

DISCUSSION

Apoptosis occurs in response to various cellular stresses or signals. In the context of myocardial ischemia, apoptosis plays a crucial role in the pathogenesis of cardiac injury, re-modeling, and dysfunction.[18] Ischemia-induced apoptosis occurs in cardiac tissues including cardiomyocytes, vascular, and other cells and is triggered by a combination of factors, including oxidative stress, calcium overload, and mitochondrial dysfunction.[18,19] These cellular events lead to the activation of specific signaling pathways that ultimately result in the activation of caspases, a family of enzymes that play a central role in the execution of apoptosis. The induction of apoptosis in the heart during myocardial ischemia contributes to the loss of viable myocardium, impairs contractile function, and may lead to heart failure.[18] Understanding the molecular mechanisms underlying ischemia-induced apoptosis in the heart is critical for the development of effective therapies aimed at reducing cardiac damage and preserving heart function. TUNEL staining marks the 3′-hydroxyl termini in the double-strand DNA breaks and is one of the most reliably ways to identify apoptosis.[20]

The TUNEL data from our study shows a significant decrease in the ratio of TUNEL positive nuclei to TUNEL negative nuclei in the ischemic myocardium of the HEV group compared with the ischemic myocardium of the CON group. This represents an overall reduction in total apoptosis in the HEV group compared to control. To further understand how EVs are changing apoptotic signaling pathways, we used western blot to evaluate key downstream markers for apoptosis.

HEV treatment was associated with a significant increase in anti-apoptotic pBAD and an increase in the pBcl-2 to Bcl-2 ratio. Phosphorylation of BAD prevents binding of BAD with Bcl-2 and Bcl-xL resulting in potent apoptotic properties.[21] Bcl-2 is known to inhibit apoptosis and studies have shown that phosphorylation of Bcl-2 results in more potent inhibition of apoptosis.[22] This increase in the ratio of pBcl-2 to Bcl-2 suggests that Bcl-2 is being phosphory-lated at an increased rate in HEV compared with CON groups.

There was a significant increase in intermediate signaling molecules pERK 1/2, ERK 1/2, pFOXO1, PI3K, and a trend towards increased pAKT and P90RSK in the HEV group

TABLE 2. Flow correlation

Marker	r	P
Flow correlation at rest		
pAKT	0.71	.09
AKT	0.12	.84
p/AKT ratio	0.86	**.02**
pBAD	−0.86	**.02**
pBCL-2	−0.43	.35
BCL-2	−0.50	.27
p/BCL-2 ratio	0.14	.78
ERK	0.25	.59
pFOXO1	−0.61	.17
FOXO1	−0.61	.17
p/FOXO1 ratio	0.50	.27
PI3K	−0.61	.17
Flow correlation with pacing		
pAKT	−0.61	.17
AKT	−0.50	.27
p/AKT ratio	−0.29	.56
pBAD	0.21	.66
pBCL-2	0.29	.56
BCL-2	0.07	.91
p/BCL-2 ratio	0.11	.84
ERK	0.11	.84
pFOXO1	0.21	.66
FOXO1	0.11	.84
p/FOXO1 ratio	−0.07	.91
PI3K	−0.25	.59

Shown is the correlation of blood flow to the ischemic myocardium at rest and while pacing at 150 beats per minute from our prior study to the expression of significant apoptotic markers in the hypoxia-conditioned extracellular vesicle group (n = 7).[10] Table shows correlation coefficient (r) and *P*-values calculated using the Spearman rank correlation coefficient. *P* values less than .05 are shown in bold. *pAKT*, Phospho-protein kinase B; *AKT*, protein kinase B; *pBAD*, phospho-Bcl-2-associated death promoter; *pBcl-2*, phospho-B-cell lymphoma 2; *Bcl-2*, B-cell lymphoma 2; *ERK*, extracellular signal-regulated kinase; *pFOXO1*, phospho-forkhead box O; *FOXO1*, forkhead box O1; *PI3K*, phosphoinositide 3-kinase.

compared with CON. There was a significant increase in the ratio of pFOXO1 to FOXO1 and pAKT to AKT.

The PI3K/AKT and ERK/P90RSK pathways have both been shown to decrease apoptosis. The PI3K/AKT pathway plays a critical role in the phosphorylation of Bcl-2 and BAD resulting in decreased overall apoptosis.[23,24] The ERK/P90RSK pathway has been shown to increase BAD phosphorylation and overall apoptosis.[25-27] FOXO1 is involved in promoting apoptosis in both mitochondria-independent and dependent pathways.[28] The phosphorylation of FOXO1 inhibits it and prevents the promotion of apoptosis.[29,30]

This study therefore demonstrated that treatment with HEV results in a significant decrease in apoptosis in the ischemic myocardium of swine compared to control. This reduction in apoptosis is likely related to the phosphorylation of FOXO1, BAD and Bcl-2 by PI3K/AKT, and ERK/P90RSK pathways. However, further studies are needed to validate the exact signaling pathway responsible for decreases in apoptosis with HEV treatment.

The results from our prior study using HEVs showed a trend toward increased myocardial blood flow with HEVs compared to traditional EVs. Correlation of relative protein expression with myocardial flow at rest and while stressing the heart by pacing at 150 beats per minute showed a positive correlation between ischemic myocardial flow at rest and the ratio of pAKT to AKT in the HEV group and a negative correlation between ischemic myocardial flow at rest and the expression of pBAD. This indicates that many of the changes seen in apoptotic signaling are not correlated with myocardial blood flow.
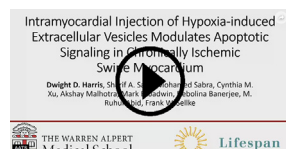
This study again demonstrates the potential for the use of EVs in the treatment of cardiovascular disease, but was not without its limitations, including sample size, marker selection, and timing of the study. This study has a relatively small sample size of 14 total swine. The sample size could result in the study being underpowered to detect changes in specific markers. Further, the study investigates a few key markers in the apoptosis pathway and could miss changes in unstudied markers or pathways. This study examines apoptosis at one fixed time point 5 weeks after EV injection, which could miss early changes related to EV injection and does not allow for collection of longer-term data. The study evaluated only one dose. Further studies are required with multiple time points and dosages to determine the full duration of benefit and optimal dosage. Furthermore, it is essential to note that all EV research is limited by the consistency of the isolated EVs. EVs are a heterogeneous group of particles, and different EVs can be derived from similar cell lines and have different products due to variations in isolation and culture techniques.[31,32] Hence, standardization, consistency, and scaling of production are crucial factors to consider as EV research continues to expand.

CONCLUSIONS

In a swine model of chronic myocardial ischemia, treatment with HEVs results in decreased overall apoptosis, which is associated with an increase in key anti-apoptotic and cell survival markers. This decrease in apoptosis could play a significant role in the increased cardiovascular benefits seen with HEV compared to traditional EVs. Further investigation is necessary to fully characterize the cardiovascular effects of HEVs, but HEVs could represent a therapeutic target for patients with chronic myocardial ischemia not amendable to traditional endovascular or surgical intervention.

Webcast 🔘

You can watch a Webcast of this AATS meeting presentation by going to: https://www.aats.org/resources/intramyocardial-injection-of-hypoxia-conditioned-extracellular-vesicles-modulates-apoptotic-signaling-in-chronically-ischemic-swine-myocardium.

Conflict of Interest Statement

The authors reported no conflicts of interest.

The *Journal* policy requires editors and reviewers to disclose conflicts of interest and to decline handling or reviewing manuscripts for which they may have a conflict of interest. The editors and reviewers of this article have no conflicts of interest.

References

1. Lindstrom M, DeCleene N, Dorsey H, Fuster V, Johnson CO, LeGrand KE, et al. Global burden of cardiovascular diseases and risks collaboration, 1990-2021. *J Am Coll Cardiol*. 2022;80:2372-425.
2. Lassaletta AD, Chu LM, Sellke FW. Therapeutic neovascularization for coronary disease: current state and future prospects. *Basic Res Cardiol*. 2011;106:897-909.
3. Knuuti J, Wijns W, Saraste A, Capodanno D, Barbato E, Funck-Brentano C, et al. 2019 ESC guidelines for the diagnosis and management of chronic coronary syndromes. *Eur Heart J*. 2020;41:407-77.
4. Jeppesen DK, Fenix AM, Franklin JL, Higginbotham JN, Zhang Q, Zimmerman LJ, et al. Reassessment of exosome composition. *Cell*. 2019;177:428-45.
5. Chakrabortty SK, Prakash A, Nechooshtan G, Hearn S, Gingeras TR. Extracellular vesicle-mediated transfer of processed and functional RNY5 RNA. *RNA*. 2015;21:1966-79. https://doi.org/10.1261/rna.053629.115
6. Karbasiafshar C, Sellke FW, Abid MR. Mesenchymal stem cell-derived extracellular vesicles in the failing heart: past, present, and future. *Am J Physiol Heart Circ Physiol*. 2021;320:H1999-2010.
7. Mathieu M, Martin-Jaular L, Lavieu G, Théry C. Specificities of secretion and uptake of exosomes and other extracellular vesicles for cell-to-cell communication. *Nat Cell Biol*. 2019;21:9-17.
8. Alibhai FJ, Tobin SW, Yeganeh A, Weisel RD, Li R-K. Emerging roles of extracellular vesicles in cardiac repair and rejuvenation. *Am J Physiol Heart Circ Physiol*. 2018;315:H733-44.
9. Potz BA, Scrimgeour LA, Pavlov VI, Sodha NR, Abid MR, Sellke FW. Extracellular vesicle injection improves myocardial function and increases angiogenesis in a swine model of chronic ischemia. *J Am Heart Assoc*. 2018;7:e008344.
10. Sabe SA, Xu CM, Potz BA, Malhotra A, Sabra M, Harris DD, et al. Comparative analysis of normoxia- and hypoxia-modified extracellular vesicle therapy in function, perfusion, and collateralization in chronically ischemic myocardium. *Int J Mol Sci*. 2023;24:2076.
11. Scrimgeour LA, Potz BA, Aboul Gheit A, Shi G, Stanley M, Zhang Z, et al. Extracellular vesicles promote arteriogenesis in chronically ischemic myocardium in the setting of metabolic syndrome. *J Am Heart Assoc*. 2019;8:012617.
12. Sabe SA, Scrimgeour LA, Xu CM, Sabra M, Karbasiafshar C, Aboulgheit A, et al. Extracellular vesicle therapy attenuates antiangiogenic signaling in ischemic myocardium of swine with metabolic syndrome. *J Thorac Cardiovasc Surg*. 2023;166:e5-14.
13. Pulido-Escribano V, Torrecillas-Baena B, Camacho-Cardenosa M, Dorado G, Gálvez-Moreno MÁ, Casado-díaz A. Role of hypoxia preconditioning in therapeutic potential of mesenchymal stem-cell-derived extracellular vesicles. *World J Stem Cells*. 2022;14:453-72.
14. Zhu J, Lu K, Zhang N, Zhao Y, Ma Q, Shen J, et al. Myocardial reparative functions of exosomes from mesenchymal stem cells are enhanced by hypoxia treatment of the cells via transferring MicroRNA-210 in an NSMase2-dependent way. *Artif Cells Nanomed Biotechnol*. 2018;46:1659-70.
15. Mao CY, Zhang TT, Li DJ, Zhou E, Fan YQ, He Q, et al. Extracellular vesicles from hypoxia-preconditioned mesenchymal stem cells alleviates myocardial injury by targeting thioredoxin-interacting protein-mediated hypoxia-Inducible factor-1α pathway. *World J Stem Cells*. 2022;14:183-99.
16. Xu CM, Karbasiafshar C, Brinck Teixeira R, Ahsan N, Blume Corssac G, Sellke FW, et al. Proteomic assessment of hypoxia-pre-conditioned human bone marrow mesenchymal stem cell-derived extracellular vesicles demonstrates promise in the treatment of cardiovascular disease. *Int J Mol Sci*. 2023;24:1674.
17. Sabe SA, Xu CM, Sabra M, Harris DD, Malhotra A, Aboulgheit A, et al. Canagliflozin improves myocardial perfusion, fibrosis, and function in a swine model of chronic myocardial ischemia. *J Am Heart Assoc*. 2023;12:e028623.
18. Kim NH, Kang PM. Apoptosis in cardiovascular diseases: mechanism and clinical implications. *Korean Circ J*. 2010;40:299-305.
19. Dhalla NS, Shah AK, Adameova A, Bartekova M. Role of oxidative stress in cardiac dysfunction and subcellular defects due to ischemia-reperfusion injury. *Biomedicines*. 2022;10:1473.
20. Kyrylkova K, Kyryachenko S, Leid M, Kioussi C. Detection of apoptosis by TUNEL assay. *Methods Mol Biol*. 2012;887:41-7.
21. Stickles XB, Marchion DC, Bicaku E, Al Sawah E, Abbasi F, Xiong Y, et al. BAD-mediated apoptotic pathway is associated with human cancer development. *Int J Mol Med*. 2015;35:1081-7.
22. Ruvolo PP, Deng X, May WS. Phosphorylation of Bcl2 and regulation of apoptosis. *Leukemia*. 2001;15:515-22.
23. Zha J, Harada H, Yang E, Jockel J, Korsmeyer SJ. Serine phosphorylation of death agonist BAD in response to survival factor results in binding to 14-3-3 not BCL-X(L). *Cell*. 1996;87:619-28.
24. Zhou H, Li XM, Meinkoth J, Pittman RN. Akt regulates cell survival and apoptosis at a postmitochondrial level. *J Cell Biol*. 2000;151:483-94.
25. Hafeez S, Urooj M, Saleem S, Gillani Z, Shaheen S, Qazi MH, et al. BAD, a proapoptotic protein, escapes ERK/RSK phosphorylation in deguelin and siRNA-treated HeLa cells. *PLoS One*. 2016;11:e0145780.
26. Hayakawa J, Ohmichi M, Kurachi H, Kanda Y, Hisamoto K, Nishio Y, et al. Inhibition of BAD phosphorylation either at serine 112 via extracellular signal-regulated protein kinase cascade or at serine 136 via Akt cascade sensitizes human ovarian cancer cells to cisplatin. *Cancer Res*. 2000;60:5988-94.
27. She QB, Solit DB, Ye Q, O'Reilly KE, Lobo J, Rosen N. The BAD protein integrates survival signaling by EGFR/MAPK and PI3K/Akt kinase pathways in PTEN-deficient tumor cells. *Cancer Cell*. 2005;8:287-97.
28. Fu Z, Tindall DJ. FOXOs, cancer and regulation of apoptosis. *Oncogene*. 2008;27:2312-9.
29. Wang T, Zhao H, Gao H, Zhu C, Xu Y, Bai L, et al. Expression and phosphorylation of FOXO1 influences cell proliferation and apoptosis in the gastrointestinal stromal tumor cell line GIST-T1. *Exp Ther Med*. 2018;15:3197-202.
30. Zhang X, Tang N, Hadden TJ, Rishi AK. Akt, FoxO and regulation of apoptosis. *Biochim Biophys Acta*. 2011;1813:1978-86.
31. Gandham S, Su X, Wood J, Nocera AL, Alli SC, Milane L, et al. Technologies and standardization in research on extracellular vesicles. *Trends Biotechnol*. 2020;38:1066-98.
32. Ng CY, Kee LT, Al-Masawa ME, Lee QH, Subramaniam T, Kok D, et al. Scalable production of extracellular vesicles and its therapeutic values: a review. *Int J Mol Sci*. 2022;23:7986.

Key Words: apoptosis, extracellular vesicle, chronic coronary artery disease, chronic myocardial ischemia, hypoxia-conditioned, swine